

New Measurement of $\frac{\text{BR}(D^+ \rightarrow \rho^0 \mu^+ \nu)}{\text{BR}(D^+ \rightarrow \bar{K}^{*0} \mu^+ \nu)}$ Branching Ratio

The FOCUS Collaboration ¹

J. M. Link ^a P. M. Yager ^a J. C. Anjos ^b I. Bediaga ^b
C. Castromonte ^b A. A. Machado ^b J. Magnin ^b A. Massafferri ^b
J. M. de Miranda ^b I. M. Pepe ^b E. Polycarpo ^b A. C. dos Reis ^b
S. Carrillo ^c E. Casimiro ^c E. Cuautle ^c A. Sánchez-Hernández ^c
C. Uribe ^c F. Vázquez ^c L. Agostino ^d L. Cinquini ^d
J. P. Cumalat ^d B. O'Reilly ^d I. Segoni ^d K. Stenson ^d
J. N. Butler ^e H. W. K. Cheung ^e G. Chiodini ^e I. Gaines ^e
P. H. Garbincius ^e L. A. Garren ^e E. Gottschalk ^e P. H. Kasper ^e
A. E. Kreymer ^e R. Kutschke ^e M. Wang ^e L. Benussi ^f
M. Bertani ^f S. Bianco ^f F. L. Fabbri ^f S. Pacetti ^f A. Zallo ^f
M. Reyes ^g C. Cawfield ^h D. Y. Kim ^h A. Rahimi ^h J. Wiss ^h
R. Gardner ⁱ A. Kryemadhi ⁱ Y. S. Chung ^j J. S. Kang ^j
B. R. Ko ^j J. W. Kwak ^j K. B. Lee ^j K. Cho ^k H. Park ^k
G. Alimonti ^l S. Barberis ^l M. Boschini ^l A. Cerutti ^l
P. D'Angelo ^l M. DiCorato ^l P. Dini ^l L. Edera ^l S. Erba ^l
P. Inzani ^l F. Leveraro ^l S. Malvezzi ^l D. Menasce ^l
M. Mezzadri ^l L. Moroni ^l D. Pedrini ^l C. Pontoglio ^l F. Prelz ^l
M. Rovere ^l S. Sala ^l T. F. Davenport III ^m V. Arena ⁿ G. Boca ⁿ
G. Bonomi ⁿ G. Gianini ⁿ G. Liguori ⁿ D. Lopes Pegna ⁿ
M. M. Merlo ⁿ D. Pantea ⁿ S. P. Ratti ⁿ C. Riccardi ⁿ P. Vitulo ⁿ
C. Göbel ^o J. Olatora ^o H. Hernandez ^p A. M. Lopez ^p
H. Mendez ^p A. Paris ^p J. Quinones ^p J. E. Ramirez ^p Y. Zhang ^p
J. R. Wilson ^q T. Handler ^r R. Mitchell ^r D. Engh ^s M. Hosack ^s
W. E. Johns ^s E. Luiggi ^s J. E. Moore ^s M. Nehring ^s
P. D. Sheldon ^s E. W. Vaandering ^s M. Webster ^s M. Sheaff ^t

^aUniversity of California, Davis, CA 95616

^bCentro Brasileiro de Pesquisas Físicas, Rio de Janeiro, RJ, Brazil

- ^c*CINVESTAV, 07000 México City, DF, Mexico*
^d*University of Colorado, Boulder, CO 80309*
^e*Fermi National Accelerator Laboratory, Batavia, IL 60510*
^f*Laboratori Nazionali di Frascati dell'INFN, Frascati, Italy I-00044*
^g*University of Guanajuato, 37150 Leon, Guanajuato, Mexico*
^h*University of Illinois, Urbana-Champaign, IL 61801*
ⁱ*Indiana University, Bloomington, IN 47405*
^j*Korea University, Seoul, Korea 136-701*
^k*Kyungpook National University, Taegu, Korea 702-701*
^l*INFN and University of Milano, Milano, Italy*
^m*University of North Carolina, Asheville, NC 28804*
ⁿ*Dipartimento di Fisica Nucleare e Teorica and INFN, Pavia, Italy*
^o*Pontificia Universidade Católica, Rio de Janeiro, RJ, Brazil*
^p*University of Puerto Rico, Mayaguez, PR 00681*
^q*University of South Carolina, Columbia, SC 29208*
^r*University of Tennessee, Knoxville, TN 37996*
^s*Vanderbilt University, Nashville, TN 37235*
^t*University of Wisconsin, Madison, WI 53706*

Abstract

Using data collected by the FOCUS experiment at Fermilab, we present a new measurement of the charm semileptonic branching ratio $\frac{\text{BR}(D^+ \rightarrow \rho^0 \mu^+ \nu)}{\text{BR}(D^+ \rightarrow \bar{K}^{*0} \mu^+ \nu)}$. From a sample of 320 ± 44 and 11372 ± 161 $D^+ \rightarrow \rho^0 \mu^+ \nu$ and $D^+ \rightarrow \bar{K}^{*0} \mu^+ \nu$ events respectively, we find $\frac{\text{BR}(D^+ \rightarrow \rho^0 \mu^+ \nu)}{\text{BR}(D^+ \rightarrow \bar{K}^{*0} \mu^+ \nu)} = 0.041 \pm 0.006$ (stat) ± 0.004 (syst).

1 Introduction

Semileptonic decays provide an ideal environment for the study of hadronic processes since the weak part of the current can be separated from the strong part of the current, and the hadronic current, described by form factors, can be calculated by Lattice QCD (Latt), Quark Model (QM), QCD Sum Rules (SR), etc. without the added complication of significant final state interactions. The importance of charm Cabibbo suppressed decays ($c \rightarrow d$) lies in their relation, through Heavy Quark Symmetry, to the decays ($b \rightarrow u$). Precise determination of these form factors can lead to a more accurate model-independent

¹ See <http://www-focus.fnal.gov/authors.html> for additional author information.

determination of $|V_{ub}|$. Previous measurements of $\frac{\text{BR}(D^+ \rightarrow \rho^0 \mu^+ \nu)}{\text{BR}(D^+ \rightarrow \bar{K}^{*0} \mu^+ \nu)}$ have suffered from lack of statistics [1,2,3], while theoretical predictions differ by at least 2σ from the world average [4]. In this paper, we present a new measurement of this branching ratio based on $320 \pm 44 D^+ \rightarrow \rho^0 \mu^+ \nu$ events.²

2 Event Selection

The data for this analysis were collected by the FOCUS experiment during the 1996–97 fixed target run at Fermilab. The FOCUS experiment utilized an upgraded version of the forward multi-particle spectrometer used by experiment E687 [5] to study charmed particles produced by the interaction of high energy photons, with average energy of ~ 180 GeV, with a segmented BeO target. Precise vertexing was made possible by two sets of silicon strips detectors consisting of two pairs of planes interleaved with the target segments [6] and four sets of planes downstream of the target region, each with three views. Five sets of proportional wire chambers combined with two oppositely polarized analysis magnets completed the tracking and momentum measurement system. Charged hadron identification was provided with three threshold multi-cell Čerenkov counters capable of separating kaons from pions up to 60 GeV/c [7]. Muons were identified in the inner muon system, located at the end of the spectrometer, which consisted of six arrays of scintillation counters subtending approximately ± 45 mrad [8].

The $D^+ \rightarrow \rho^0 \mu^+ \nu$ events are selected by requiring two oppositely charged pions and a muon to form a good decay vertex with confidence level exceeding 5%. Tracks not used in the decay vertex are used to form candidate production vertices. Of these candidates, the vertex with the highest multiplicity is selected as the production vertex; ties are broken by selecting the most upstream vertex. This production vertex is required to have a confidence level greater than 1% and be inside the target material.

Muon tracks are required to have a minimum momentum of 10 GeV/c and must have hits in at least five of the six planes comprising the inner muon system. These hits must be consistent with the muon track hypothesis with a confidence level exceeding 1%. In order to reduce contamination from in-flight decay of pions and kaons within the spectrometer, we require the muon tracks to have a confidence level greater than 1% under the hypothesis that the trajectory is consistent through the two analysis magnets.

The Čerenkov algorithm used for particle identification returns the negative log-likelihood for a given track to be either an electron, pion, kaon or proton. To identify the two pion candidates we require that no other hypothesis is

² Unless stated otherwise, charge conjugation is implied

favored over the pion hypothesis by more than five units of log-likelihood for each track. Furthermore, we require that the pion hypothesis for the track with charge opposite to the muon be favored over the kaon hypothesis by at least five units of log-likelihood. This is a very stringent cut used to suppress background from the Cabibbo favored decay $D^+ \rightarrow K^- \pi^+ \mu^+ \nu$ where the kaon is misidentified as a pion. Additionally, the pion hypothesis must be favored over the kaon hypothesis by more than one unit of log-likelihood for the remaining track.

To suppress short-lived backgrounds, we require the decay vertex to be separated from the production vertex by at least 15 times the error of the separation σ_L and be out of the target material by 1σ . Because the target region has embedded detectors, the decay vertex is also required to be outside the detector material. These cuts are especially effective at removing non-charm backgrounds, making the contribution from minimum-bias events negligible. Contamination from higher multiplicity charm events is reduced by isolating the $\pi\pi\mu$ vertex from other tracks in the event (not including tracks in the primary). We require that the maximum confidence level for any other track to form a vertex with the candidate to be less than 1%.

Background from $D^{*+} \rightarrow D^0 \pi^+ \rightarrow (\pi^- \mu^+ \nu) \pi^+$, where the soft pion is erroneously assigned to the decay vertex, is reduced by requiring $M(\pi^+ \pi^- \mu^+) - M(\pi^- \mu^+) > 0.20 \text{ GeV}/c^2$. Background decay modes with a neutral hadron in the final state, such as $D_s^+ \rightarrow \eta' \mu^+ \nu \rightarrow (\eta \pi^+ \pi^+) \mu^+ \nu$, are reduced by requiring a visible mass cut of $1.2 \text{ GeV}/c^2 < M(\pi^+ \pi^- \mu^+) < 1.8 \text{ GeV}/c^2$. This cut eliminates $\sim 40\%$ of the $D^+ \rightarrow \rho^0 \mu^+ \nu$ signal, but also proves to be very effective at rejecting background consisting mostly of kaons and pions misidentified as muons.

In reconstructing the $D^+ \rightarrow K^- \pi^+ \mu^+ \nu$ events used for normalization, we use the same vertex and muon identification cuts as in the $D^+ \rightarrow \rho^0 \mu^+ \nu$ analysis. The kaon is identified by requiring that the kaon hypothesis is favored over the pion hypothesis by at least two units of log-likelihood. The pion candidate is identified by requiring that the pion hypothesis for this track be favored over the kaon hypothesis. Background from $D^{*+} \rightarrow D^0 \pi^+ \rightarrow (K^- \mu^+ \nu) \pi^+$ is reduced by requiring $M(K^- \pi^+ \mu^+) - M(K^- \mu^+) > 0.20 \text{ GeV}/c^2$. A cut on the visible mass of $1.0 \text{ GeV}/c^2 < M(K^- \pi^+ \mu^+) < 1.8 \text{ GeV}/c^2$ suppresses background from muon misidentification.

3 BR Determination

The $D^+ \rightarrow \rho^0 \mu^+ \nu$ yield is estimated using a binned maximum log-likelihood fit of the $\pi^+ \pi^-$ invariant mass. The likelihood is defined as:

$$\mathcal{L} = \prod_{i=1}^{\text{\#bins}} \frac{n_i^{s_i} e^{-n_i}}{s_i!} \quad (1)$$

$$n_i = Y_{D^+ \rightarrow \rho^0 \mu^+ \nu} S_{1i} + \text{ECY}_{D^+ \rightarrow \bar{K}^{*0} \mu^+ \nu} \epsilon(\bar{K}^{*0} \mu^+ \nu \rightarrow \rho \mu \nu) S_{2i} + Y_{D^+ \rightarrow K_S^0 \mu^+ \nu} S_{3i} + Y_{D^+ \rightarrow \omega \mu^+ \nu} S_{4i} + Y_{D_s^+} S_{5i} + \mathcal{C} S_{6i} + \mathcal{M} S_{7i} \quad (2)$$

where s_i is the number of events in bin i of the data histogram and n_i is the number of events in bin i of the fit histogram.

The fit histogram is composed of the $D^+ \rightarrow \rho^0 \mu^+ \nu$ signal and background decay shapes. The background shapes include charm semileptonic decays, combinatorial background where at least one of the three charged tracks used in the decay vertex does not belong to the vertex, and background from muon misidentification. The charm semileptonic backgrounds considered are $D^+ \rightarrow K^- \pi^+ \mu^+ \nu$, where the kaon is misidentified as a pion, $D^+ \rightarrow K_S^0 \mu^+ \nu$, $D^+ \rightarrow \omega \mu^+ \nu$ where the ω could decay either to $\pi^+ \pi^- \pi^0$ or $\pi^+ \pi^-$, and various semileptonic D_s^+ modes with two pions and one neutral hadron in the final state. In Eq. 2 the S_{ni} are normalized shapes from Monte Carlo samples and the parameters Y_x , \mathcal{C} , and \mathcal{M} are fit parameters. The efficiency-corrected yield (ECY) for $D^+ \rightarrow \bar{K}^{*0} \mu^+ \nu$ is fixed in the fit to the value obtained from the $D^+ \rightarrow K^- \pi^+ \mu^+ \nu$ analysis used for the normalization mode and $\epsilon(\bar{K}^{*0} \mu^+ \nu \rightarrow \rho \mu \nu)$ is the efficiency for a $D^+ \rightarrow \bar{K}^{*0} \mu^+ \nu$ event to be reconstructed as a $D^+ \rightarrow \rho^0 \mu^+ \nu$ event. The D_s^+ yield is the sum of the modes $D_s^+ \rightarrow \eta' \mu \nu$, $D_s^+ \rightarrow \eta \mu \nu$, and $D_s^+ \rightarrow \phi \mu^+ \nu$ with $\eta' \rightarrow \rho^0 \gamma$ and $\eta' \rightarrow \eta \pi^+ \pi^-$, $\eta \rightarrow \pi^+ \pi^- \pi^0$ and $\eta \rightarrow \pi^+ \pi^- \gamma$, and $\phi \rightarrow \rho \pi$. We use the recent CLEO-c collaboration measurements of the absolute branching ratio of $D^+ \rightarrow \bar{K}^{*0} e^+ \nu$ and $D^+ \rightarrow \omega e^+ \nu$ [9] to set a loose constraint on the yield of $D^+ \rightarrow \omega \mu^+ \nu$. To this end, we add a penalty term to the likelihood of the form³

$$\exp \left[-\frac{1}{2} \left(R_{\omega/\bar{K}^{*0}} \text{ECY}_{D^+ \rightarrow \bar{K}^{*0} \mu^+ \nu} - Y_{D^+ \rightarrow \omega \mu^+ \nu} \right)^2 / \sigma_{D^+ \rightarrow \omega e \nu}^2 \right] \quad (3)$$

where $R_{\omega/\bar{K}^{*0}} = \frac{\text{BR}(D^+ \rightarrow \omega e^+ \nu)}{\text{BR}(D^+ \rightarrow \bar{K}^{*0} e^+ \nu)}$.

The $\sigma_{D^+ \rightarrow \omega e \nu}$ error used in Eq. 3 is based on the errors in the branching fractions reported by CLEO-c with statistical and systematic errors added in

³ Here we have assumed that the electronic and muonic rates are equal.

quadrature to the error in the efficiency corrected yield for $D^+ \rightarrow \bar{K}^{*0} \mu^+ \nu$. Fig. 2 shows the shapes of the semileptonic contributions used in the fit. Both the D_s^+ and the $D^+ \rightarrow \omega \mu^+ \nu$ shapes are doubly peaked. The muon misidentification and combinatorial background are described below.

The muon misidentification shape is obtained from a large $c\bar{c}$ Monte Carlo sample with all known charm decays where tracks within the acceptance of the inner muon system with a confidence level less than 1% and momentum greater than 10 GeV/ c are taken as muons. This allows us to use the same selection as in the analysis, but with very few real semi-muonic decays in the sample. This shape is then weighted with a momentum-dependent misidentification probability function to obtain the final shape used in the fit. The combinatorial background is also obtained from a large $c\bar{c}$ Monte Carlo sample where after an event is selected the reconstructed tracks are matched against the generated tracks. If the reconstructed tracks do not belong to the same vertex, the event is flagged as a combinatorial event.

The $D^+ \rightarrow K^- \pi^+ \mu^+ \nu$ yield used for the normalization is estimated in the same way as the $D^+ \rightarrow \rho^0 \mu^+ \nu$ yield. In this case, we only need two components in the fit: one for the signal and one for the background. This background shape is obtained from a Monte Carlo sample where all known charm decays, except $D^+ \rightarrow K^- \pi^+ \mu^+ \nu$, are generated. This fit to the $K^- \pi^+$ line shape is similar to the one used in [10], and though this fit does not describe the complex line shape presented in [11], we find that it provides a robust estimate of the $D^+ \rightarrow K^- \pi^+ \mu^+ \nu$ yield.

From our fit we find 320 ± 44 $D^+ \rightarrow \rho^0 \mu^+ \nu$ events and $11,372 \pm 161$ $D^+ \rightarrow K^- \pi^+ \mu^+ \nu$ events. Fig. 1 shows the fit result. The branching ratio is defined as

$$\frac{\text{BR}(D^+ \rightarrow \rho^0 \mu^+ \nu)}{\text{BR}(D^+ \rightarrow \bar{K}^{*0} \mu^+ \nu)} = \frac{Y_{D^+ \rightarrow \rho^0 \mu^+ \nu} / \epsilon_{D^+ \rightarrow \rho^0 \mu^+ \nu}}{Y_{D^+ \rightarrow K^- \pi^+ \mu^+ \nu} / \epsilon_{D^+ \rightarrow K^- \pi^+ \mu^+ \nu}} \times \text{BR}(\bar{K}^{*0} \rightarrow K^- \pi^+). \quad (4)$$

This branching ratio must be corrected to account for the $(5.30 \pm 0.74_{-0.96}^{+0.99})\%$ non-resonant S-wave contribution present in the $D^+ \rightarrow K^- \pi^+ \mu^+ \nu$ spectrum previously reported by FOCUS [8,11]. After this correction we find

$$\frac{\text{BR}(D^+ \rightarrow \rho^0 \mu^+ \nu)}{\text{BR}(D^+ \rightarrow \bar{K}^{*0} \mu^+ \nu)} = 0.0412 \pm 0.0057.$$

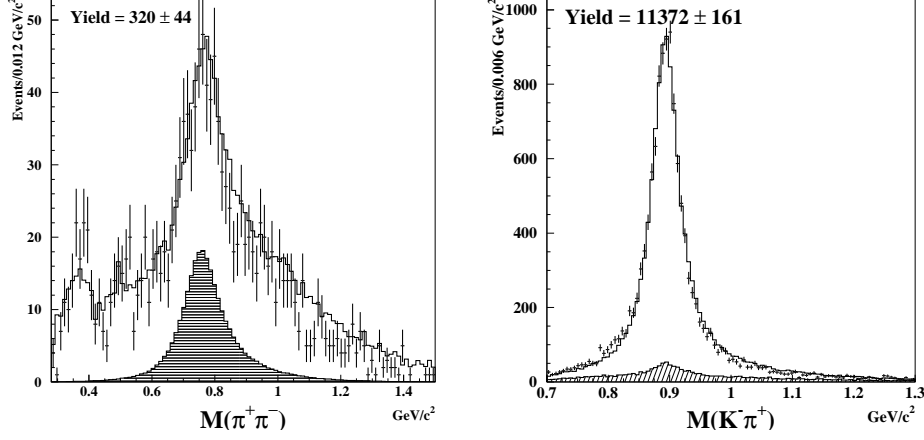


Fig. 1. Fit to the $\pi^+\pi^-$ invariant mass (left) and the $K^-\pi^+$ invariant mass (right). The fit to the data (error bars) is shown as a solid line. The hatched histogram on the $\pi^+\pi^-$ invariant mass plot is the $D^+ \rightarrow \rho^0 \mu^+ \nu$ signal contribution. The hatched histogram on the $K^-\pi^+$ invariant mass is the background.

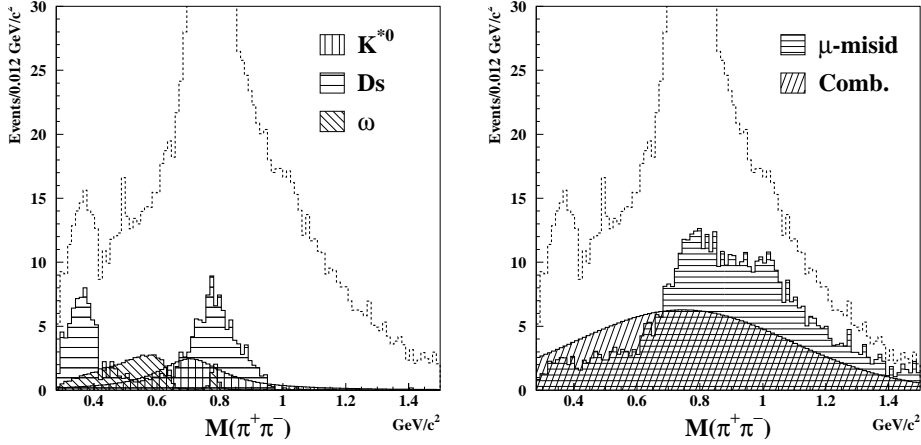


Fig. 2. $M(\pi^+\pi^-)$ background spectra. Left: semileptonic contributions. Note that both the D_s^+ as well as the ω shapes are doubly peaked. For the sake of clarity, we have omitted the $K_S^0 \rightarrow \pi^+\pi^-$ plot. Right: Muon misid and combinatorial background contributions. The dashed line represents the fit histogram. In the case of the $D^+ \rightarrow \bar{K}^{*0} \mu^+ \nu$ and combinatorial backgrounds, smoothed shapes been used.

4 Systematic Studies

Several studies have been performed in order to assess any systematic contribution to the uncertainty in the ratio. Three possible contributions have been identified.

The first contribution is due to the final cut selection used to determine the branching ratio. This systematic is assessed by measuring the branching ratio for different cut combinations and calculating the sample variance for the

returned values of $\frac{\text{BR}(D^+ \rightarrow \rho^0 \mu^+ \nu)}{\text{BR}(D^+ \rightarrow \bar{K}^{*0} \mu^+ \nu)}$. We vary the cuts by applying more stringent cuts on the significance of the separation between the production and the decay vertices, the confidence level and out of target requirements for the decay vertex, the Čerenkov identification cuts for the pions, and the cuts used in the muon identification. Since the visible mass cut is a kinematic cut, we also performed the fit without any restriction on the visible mass. We find no significant change in the branching ratio due to our particular cut choice and assign a systematic uncertainty of 0.0023 due to our cut selection.

The second contribution is related to our fit. In order to check the fit against possible biases as well as the accuracy of the statistical error reported by the fit, we perform the fit multiple times after fluctuating each bin of the data histogram using a Poisson distribution. We find that both the mean and width of the distribution of the fit results are in agreement with our reported results.

We test the effect of the fit inputs by changing the $D^+ \rightarrow K^- \pi^+ \mu^+ \nu$ ECY used to estimate the amount of background due to K/π misidentification in our $D^+ \rightarrow \rho^0 \mu^+ \nu$ sample by $\pm 3\sigma$ and by fitting with no restrictions on the $D^+ \rightarrow \omega \mu^+ \nu$ yield. We test the combined D_s^+ shape used in the fit by fitting our signal using the individual shapes of the D_s^+ modes mentioned earlier. In this case, we replace the D_s^+ yield parameter in the fit with a parameter representing the $D_s^+ \rightarrow \phi \mu^+ \nu$ ECY and we extract the individual yields using the branching ratios of these modes relative to $D_s^+ \rightarrow \phi \mu^+ \nu$. These branching ratios are then varied by $\pm 1\sigma$. We have also changed the shape of the combinatorial background by replacing it with the shape obtained when two same sign pions are used to form a $\pi\pi\mu$ vertex. As a final check on the fit, we have changed the binning scheme and mass range used in the fit. As in the case of cut variations, we calculate the sample variance of the returned values and quote this as our systematic contribution. We find this contribution to be 0.0038 mostly coming from the uncertainty in the combinatorial background shape.

The third category includes possible systematic effects from the detector simulation and the charm production mechanism. We estimate this by splitting our sample into three pairs of statistically independent sub-samples according to the D^\pm momentum, whether we have a decay of a D^+ or a D^- , and whether the upstream silicon strip detector was installed or not. In order to assess the likely systematic error contribution in any differences in the results from larger statistical fluctuations due to reduced statistics, FOCUS uses a technique based on the *S-factor* method of the PDG. In this method the branching ratio is measured for each pair of sub-samples and a scaled variance is calculated. The split sample contribution is the difference between the scaled variance and the statistical variance if the scaled variance is greater than the statistical variance for the un-split sample. We find no contribution to the systematic uncertainty from this source.

The total systematic uncertainty is obtained by adding in quadrature all of

these contributions as summarized in Table 1.

Systematic Source	Error
Cut variations	0.0023
Fit variation	0.0038
Split sample	0.0000
Total	0.0044

Table 1

Sources of systematic errors. The three sources are added in quadrature to obtain the total systematic error.

5 Conclusions

From $320 \pm 44 D^+ \rightarrow \rho^0 \mu^+ \nu$ decays and $11,372 \pm 161 D^+ \rightarrow K^- \pi^+ \mu^+ \nu$ decays, we report a measurement of the branching ratio

$$\frac{\text{BR}(D^+ \rightarrow \rho^0 \mu^+ \nu)}{\text{BR}(D^+ \rightarrow \bar{K}^{*0} \mu^+ \nu)} = 0.041 \pm 0.006 \text{ (stat.)} \pm 0.004 \text{ (syst.)}.$$

Using this result along with the FOCUS measurement of the ratio $\frac{\text{BR}(D^+ \rightarrow \bar{K}^{*0} \mu^+ \nu)}{\text{BR}(D^+ \rightarrow K^- \pi^+ \pi^+)}$ [12], the PDG value of the absolute branching fraction of the decay $D^+ \rightarrow K^- \pi^+ \pi^+$, and the FOCUS measurement of the D^+ lifetime [13], we calculate

$$\Gamma(D^+ \rightarrow \rho^0 \mu^+ \nu) = (0.22 \pm 0.03 \pm 0.02 \pm 0.01) \times 10^{10} \text{ s}^{-1}$$

where the last error is a combination of the uncertainties on the quantities not measured in this work. When calculating the decay partial width, we have corrected the $\frac{\text{BR}(D^+ \rightarrow \bar{K}^{*0} \mu^+ \nu)}{\text{BR}(D^+ \rightarrow K^- \pi^+ \pi^+)}$ with the updated value for the S-wave non-resonant contribution. In Table 2 and Table 3, we compare our result to previous experimental results and theoretical predictions, respectively.

This result is consistent with a recent CLEO collaboration result on the absolute branching ratios for D^+ semileptonic decays [9] and represents a significant improvement to the PDG world average. This result also indicates that the QCD Sum Rule predictions [14,15] are too low.

6 Acknowledgments

We wish to acknowledge the assistance of the staffs of Fermi National Accelerator Laboratory, the INFN of Italy, and the physics departments of the

Reference	$\frac{\text{BR}(D^+ \rightarrow \rho^0 \mu^+ \nu)}{\text{BR}(D^+ \rightarrow \bar{K}^{*0} \mu^+ \nu)}$	$\frac{\text{BR}(D^+ \rightarrow \rho^0 e^+ \nu)}{\text{BR}(D^+ \rightarrow \bar{K}^{*0} e^+ \nu)}$
E653 [1]	$0.044^{+0.034}_{-0.029}$	
E687 [2]	0.079 ± 0.023	
E791 [3]	0.051 ± 0.017	0.045 ± 0.017
CLEO [9]		0.038 ± 0.008
This result	0.041 ± 0.007	

Table 2

Experimental results for the branching ratio. Statistical and systematic errors have been added in quadrature.

Reference	ℓ	$\frac{\text{BR}(D^+ \rightarrow \rho^0 \ell^+ \nu)}{\text{BR}(D^+ \rightarrow \bar{K}^{*0} \ell^+ \nu)}$	$\Gamma(D^+ \rightarrow \rho^0 \ell^+ \nu)(10^{10} \text{ s}^{-1})$
Ball [14] (SR)	e		0.06 ± 0.02
APE [16] (Latt)	ℓ	0.043 ± 0.018	0.3 ± 0.1
Jaus [17] (QM)	ℓ	0.030	0.16
ISGW2 [18] (QM)	e	0.023	0.12
Yang–Hwang [15] (SR)	e	0.018 ± 0.005	$0.07^{+0.04}_{-0.02}$
O’Donnell–Turan [19] (LF)	μ	0.025	
Melikhov [20] (QM)	ℓ	0.027, 0.024	0.15, 0.13
Kondratyuk–Tchein [21] (LF)	ℓ	0.035, 0.033, 0.033, 0.032	0.19, 0.20, 0.18, 0.19
Melikhov–Stech [22] (QM)	ℓ	0.035	0.21
Wang–Wu–Zhong [23] (LC)	ℓ	0.035 ± 0.011	0.17 ± 0.04
This result	μ	0.041 ± 0.008	0.21 ± 0.04

Table 3

Theoretical predictions for the branching ratio and partial decay width. Most of the theoretical predictions are calculated for $D^0 \rightarrow \rho^- l^+ \nu$. To compare these predictions with our result, we have used the isospin conjugate relation $\Gamma(D^+ \rightarrow \rho^0 l^+ \nu) = 1/2 \Gamma(D^0 \rightarrow \rho^- l^+ \nu)$.

collaborating institutions. This research was supported in part by the U. S. National Science Foundation, the U. S. Department of Energy, the Italian Istituto Nazionale di Fisica Nucleare and Ministero dell’Università e della Ricerca Scientifica e Tecnologica, the Brazilian Conselho Nacional de Desenvolvimento Científico e Tecnológico, CONACyT-México, the Korean Ministry of Education, and the Korea Research Foundation.

References

- [1] K. Kodama et al., Observation of $D^+ \rightarrow \rho(770)^0 \mu^+ \nu$, Phys. Lett. B 316 (1993) 455.
- [2] P. L. Frabetti et al., Observation of the Vector Meson Cabibbo Suppressed Decay $D^+ \rightarrow \rho^0 \mu^+ \nu$, Phys. Lett. B 391 (1997) 235.
- [3] E. M. Aitala et al., Measurement of the Branching Ratio $\frac{B(D^+ \rightarrow \rho^0 l^+ \nu_l)}{B(D^+ \rightarrow K^{*0} l^+ \nu_l)}$, Phys. Lett. B 397 (1997) 325.
- [4] S. Eidelman et al., Review of Particle Physics, Phys Lett. B 592 (2004) 1.
- [5] P. L. Frabetti et al., Description and Performance of the Fermilab E687 Spectrometer, Nucl. Instrum. Meth. A 320 (1992) 519.
- [6] J. M. Link et al., The Target Silicon Detector for the FOCUS Spectrometer, Nucl. Instrum. Meth. A 516 (2004) 364.
- [7] J. M. Link et al., Čerenkov Identification in FOCUS, Nucl. Instrum. Meth. A 484 (2002) 270.
- [8] J. M. Link et al., Evidence for New Interference Phenomena in the Decay $D^+ \rightarrow K^- \pi^+ \mu^+ \nu$, Phys. Lett. B 535 (2002) 43.
- [9] G. S. Huang et al., Absolute Branching Fraction Measurements of Exclusive D^+ Semileptonic Decays, hep-ex/0506053 .
- [10] J. M. Link et al., Measurement of the Ratio of the Vector to Pseudoscalar Charm Semileptonic Decay Rate $\frac{\Gamma(D^+ \rightarrow \bar{K}^{*0} \mu^+ \nu)}{\Gamma(D^+ \rightarrow \bar{K}^0 \mu^+ \nu)}$, Phys. Lett. B 598 (2004) 33.
- [11] J. M. Link et al., Hadronic Mass Spectrum Analysis of $D^+ \rightarrow K^- \pi^+ \mu^+ \nu$ Decay and Measurement of the $K^*(892)^0$ Mass and Width, Phys. Lett. B 320 (2005) 72.
- [12] J. M. Link et al., New Measurement of the $\frac{\Gamma(D^+ \rightarrow \bar{K}^{*0} \mu^+ \nu)}{\Gamma(D^+ \rightarrow K^- \pi^+ \pi^+)}$ and $\frac{\Gamma(D_S^+ \rightarrow \phi \mu^+ \nu)}{\Gamma(D_S^+ \rightarrow \phi \pi^+)}$, Phys. Lett. B 541 (2002) 243.
- [13] J. M. Link et al., New Measurement of the D^0 and D^+ lifetimes, Phys. Lett. B 537 (2002) 192.
- [14] P. Ball, Semileptonic Decays $D \rightarrow \pi(\rho) e \nu$ and $B \rightarrow \pi(\rho) e \nu$ from QCD Sum Rules, Phys. Rev. D 48 (1993) 3190.
- [15] W. Y. Wang, Y. L. Wu and M. Zhong, The QCD Sum Rule Approach for the Semileptonic Decay of the D or B Meson into a light meson and leptons, Z. Phys, C 73 (1997) 275.
- [16] C. R. Allton et al., Lattice Calculation of D and B Meson Semileptonic Decays, Using the Clover Action at $\beta = 6.0$ on APE, Phys. Lett. B 345 (1995) 513.
- [17] W. Jaus, Semileptonic, Radiative and Pionic decays of B, B* and D, D* Mesons, Phys. Rev. D 53 (1996) 1349.

- [18] N. Igsur and D. Scora, Semileptonic Meson Decays in the Quark Model: An Update, *Phys. Rev. D* 52 (1995) 2783.
- [19] P. J. O'Donnell and G. Turan, Charm and Bottom Semileptonic Decays, *Phys. Rev. D* 56 (1997) 295.
- [20] D. Melikhov, Exclusive Semileptonic Decays of Heavy Mesons in the Quark Model, *Phys. Lett. B* 394 (1997) 385.
- [21] L. A. Kondratyuk and D. V. Tchekin, Transition Form Factors and Probabilities of the Semileptonic Decays of B and D Mesons within Covariant Light-Front Dynamics, *Phys. Atom. Nucl.* 64 (2001) 727.
- [22] D. Melikhov and B. Stech, Weak Form Factors for Heavy Meson Decays: An Update, *Phys. Rev. D* 62 (2000) 014006.
- [23] W. Y. Wang, Y. L. Wu and M. Zhong, Heavy to Light Meson Exclusive Semileptonic Decays in Effective Field Theory of Heavy Quarks, *Phys. Rev. D* 67 (2003) 014024.